



Investigation of Uridine in Anti-Aging-Related Diseases Based on Network Pharmacology, Molecular Docking and Cell Experimental Validation

Haoxin Ma,¹ Xiaowei Dai,³ Tao Wang,² Zhongmei He,¹ Rui Du,¹ Hongyan Pei,¹ Tianyuan Liu,¹ Ruifen Sun^{2,*} and Kui Zhao^{2,*}

Abstract

There is currently only literature that verifies through in vivo experiments in animals that uridine can increase the metabolic level in mice, lacking research and validation on the anti-aging mechanism of uridine. Using network pharmacology, 83 drug targets and 5758 disease targets were screened out, and 33 common targets between aging-related diseases and the selected uridine were determined, including key proteins (PLA2G2A, ADK, G6PD, and GLA). Ten core targets were screened out from the Protein-Protein Interaction network (TP53, INS, CASP3, MYC, ADA, SERPINE1, SLC2A4, DPP4, G6PD, and TYMS). Molecular docking provided further verification. The CCK-8 experiment demonstrated that uridine has a significant therapeutic effect on D-galactose-induced senescence in HT22, BV2, and PC12 cells. Biochemical index detection results indicated that uridine can reduce the content of Malondialdehyde (MDA) and the enzyme activity of Lactate Dehydrogenase (LDH) in senescent HT22, BV2, and PC12 cells, increase the enzyme activity of Superoxide dismutase (SOD), and lower the expression levels of inflammatory factors IL-1 β and TNF- α , thereby reducing the damage to HT22, BV2, and PC12 cells caused by inflammatory factors. This study highlights the potential of uridine as a source of anti-aging activity and suggests that it can be developed into a new drug for treating aging-related diseases.

Keywords: Uridine; Anti-aging; Network pharmacology; Molecular docking.

Received: 04 May 2025; Revised: 27 May 2025; Accepted: 29 May 2025.

Article type: Research article.

1. Introduction

For many years, aging has been regarded as a pathological process that easily triggers many diseases.^[1] Recently, the term "aging-related diseases" has emerged.^[2,3] There are common mechanisms between aging and the onset of these diseases, including living environment,^[4] safety of food,^[5] stress adaptation, loss of protein homeostasis, stem cell exhaustion, metabolic disorders, macromolecular damage, epigenetic modifications, and inflammatory responses.^[6-8] During the

aging process in the human body, the accumulation of molecular, cellular, and organ damage can induce a series of diseases, such as cardiovascular diseases, metabolic diseases, and neurological diseases.^[9-11] As researchers' attention grows, more and more aging markers^[12] and anti-aging substances have been discovered.^[13,14]

In recent years, with the continuous increase in the elderly population, the problems caused by aging have become increasingly serious, and there is an urgent need to discover substances that can effectively delay or even treat aging-related diseases.^[15-17] Uridine is a small molecule nucleoside composed of uracil and a ribose (furanose) ring, which belongs to the category of nucleosides and their derivatives. Uridine is the precursor of lecithin, and lecithin is an important component of cell membranes. Therefore, uridine can provide materials for cell regeneration. In the mitochondria that supply energy to cells, a large amount of lecithin is also enriched. So uridine can also provide power for cell regeneration. Studies

¹ College of Chinese Materia Medica, Jilin Agricultural University, Changchun, Jilin, 130118, China

² School of Nursing, Yunnan University of Chinese Medicine, Kunming, 650500, China

³ Reproductive Medical Center, The Second Norman Bethune Hospital of Jilin University, Changchun, Jilin, 130000, China

*Email: sunruifen@ynuucm.edu.cn (R. F. Sun);

zhaok06@ynuucm.edu.cn (K. Zhao)

have shown that cells (cancer cells, immune cells) can generally utilize uridine as a source of nutrition and energy.^[18,19]

Uridine has multiple biological functions and has been proven to have anti-aging effects in animal models, but the mechanism is still not comprehensive.^[20,21] Therefore, this article will determine the anti-aging targets of uridine through network pharmacology and verify its binding ability through molecular docking, and further confirm the anti-aging ability of uridine through cell models.

2. Research methods

2.1 Venn diagram for target intersection and drug-active component-intersection gene network

Firstly, enter the Venny website (<https://bioinfogp.cnb.csic.es/tools/venny/index.htm>), import the data corresponding to uridine and aging-related diseases to obtain the intersection targets of diseases and drugs. Input them into the drawing software DrawVenn Diagram to obtain the potential target points for uridine in the treatment of aging-related diseases. Import the component target data of uridine and aging-related diseases into the Network file, and then screen the target genes based on the p-values (Probability values > 0) of the active components. Use the Tape file to select the genes of the main drug active components and diseases, and name the main component as mol, the gene as gene, and the drug as drug. Screen gene, mol, and drug, and on this basis, construct the network relationship between "drug-active component-target".^[22]

2.2 Construction of PPI network diagram-Protein-Protein interaction network

Import the word file of the intersection targets of uridine and aging-related diseases into the STRING database (<https://string-db.org>), set parameters such as degree centrality and closeness centrality, and screen out the core targets of drugs and diseases. Input the gene targets collected in the Venny diagram into the STRING database, and set the interaction threshold between proteins to "highest confidence" (>0.9) to obtain the target interaction network diagram.

2.3 GO functional enrichment

GO enrichment analysis is an analytical method used to study specific drugs, and it is usually used to enrich the physiological mechanisms (Biological Process, BP), molecular mechanisms (Molecular Function, MF), and cellular components (Cell Component, CC) within them. Conduct GO functional enrichment analysis on the 33 intersection targets through the Metascape platform.

2.4 KEGG pathway analysis

Conduct KEGG pathway enrichment analysis on the 33 intersection targets through the Metascape platform, and draw bubble charts using the Bioinformatics Online Platform (<http://www.bioinformatics.com.cn/>).

2.5 Molecular docking

Based on the results of GO functional and KEGG pathway enrichment analysis, the top 10 are selected for molecular docking, and the top three are visualized. Collect the 2D structure information of small molecules through the PubChem database, optimize the structure of small molecules using ChemBio3D Ultra 14.0, and convert them into 3D structures. Search for the ID information of proteins through the Uniprot database, download the corresponding protein structure information from the Protein Data Bank (RCSB-PDB), and remove water and small molecules from the protein using PyMOL 3.1. Then, use AutoDockTools-1.5.7 software to add hydrogen bonds to the protein and small molecules, and search for the docking pocket information of the protein. Use Vinna software for molecular docking of the protein and small molecules. Use PyMOL 3.1 to visualize the docking results and display the interaction between the protein and small molecules.^[23]

2.6 Protective effects of uridine on D-Galactose-induced senescence in cells

2.6.1 Materials, reagents and equipment

HT-22, BV2, and PC12 mouse hippocampal neuron cells: College of Chinese Medicinal Materials, Jilin Agricultural University; Fetal bovine serum (FBS), penicillin-streptomycin, PBS: Thermo Fisher Scientific, USA; DMEM high glucose medium: Gibco, USA; D-galactose, CCK-8: Shanghai Yuanye Bio-Technology Co., Ltd.; CB150 cell culture incubator: Binder, Germany; DH100-4 dry bath incubator, microplate reader: Hangzhou Ruicheng Instrument Co., Ltd.

2.6.2 Cell culture

Cell culture conditions: HT-22, BV2, and PC12 cells were cultured in a 37° C, 5% CO₂ cell culture incubator with DMEM medium containing 10% FBS and 1% penicillin-streptomycin. Cells were passaged when they reached approximately 86% confluence.

2.6.3 CCK-8 assay

2.6.3.1 Effects of different concentrations of D-Galactose on cell viability

Cells in the logarithmic growth phase were collected and 100 μ L of cell suspension (approximately 6×10^4 cells per well)

was added to each well of a 96-well plate. The cells were cultured in a cell culture incubator for 24 hours. The supernatant was discarded, and 100 μ L of medium containing different concentrations of D-galactose (10, 50, 100 mM) was added for incubation for 24 hours. Then, 10 μ L of CCK-8 solution was directly added, and the cells were further cultured for 1 hour. Absorbance was measured at 450 nm using a microplate reader. Cell viability (Z, %) was calculated by the following Eq. (1).

$$Z = (A_{sample} - A_{blank}) / (A_{control} - A_{blank}) \times 100\% \quad (1)$$

where A_{sample} represents the absorbance of the treatment group (D-galactose, CCK-8, cells); $A_{control}$ represents the absorbance of the blank control group (CCK-8, cells); A_{blank} represents the absorbance of the control group (CCK-8).

2.6.3.2 Effects of Uridine on the viability of three types of cells

The same cell culture method as described in “Effects of different concentrations of D-Galactose on cell viability” was used. After incubation with the same concentration of cells, the supernatant was discarded, and 100 μ L of culture medium containing different concentrations of uridine (20, 30, 40, 50, 60 μ mol/L) was added and incubated for 24 hours. Then, 10 μ L of CCK-8 solution was directly added, and the cells were further cultured for 1 hour. Cell viability was determined using the CCK-8 assay.

2.6.3.3 Protective effects of uridine on D-Galactose-damaged cells

The same cell culture method as described in “Effects of different concentrations of D-Galactose on cell viability” was used. After incubation with the same concentration of cells,

HT22, BV2, and PC12 cells were cultured at an appropriate concentration of D-galactose as the model group. The supernatant was then removed, and 100 μ L of culture medium was added and incubated for 24 hours at different concentrations of uridine (20, 30, 40 μ mol/L). The blank group was normally cultured, and the model group was the D-galactose aging model selected in “Effects of different concentrations of D-Galactose on cell viability”. Cell viability was determined using the CCK-8 assay.

2.6.3.4 Biochemical index detection

The same cell culture method as described in “Protective effects of uridine on D-Galactose-damaged cells” was used. The three types of cells were first modeled and then treated. After 24 hours of continued culture, the cells and supernatant were collected, and the activities of lactate dehydrogenase (LDH) and superoxide dismutase (SOD), the content of malondialdehyde (MDA), and the levels of cytokines interleukin-1 β (IL-1 β) and tumor necrosis factor- α (TNF- α) were determined according to the instructions of the kit.

3. Results

3.1 Venn diagram targets and main component intersection gene network

3.1.1 Intersection of Venn diagram targets

By searching the GeneCards database, a total of 5758 targets related to the treatment of age-related diseases and 83 uridine gene targets were obtained. Among them, the GeneCards database selects target points with a correlation score greater than the median, resulting in a final set of 33 intersection targets after merging and deduplication. A total of 33 are potential targets for the treatment of age-related diseases with uridine. Fig. 1 shows the Venn diagram of intersecting targets.

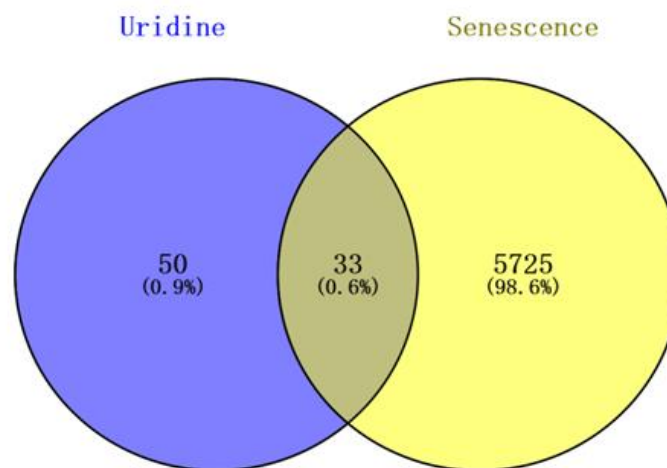


Fig. 1: Venn diagram of the intersection of uridine-aging-related diseases.

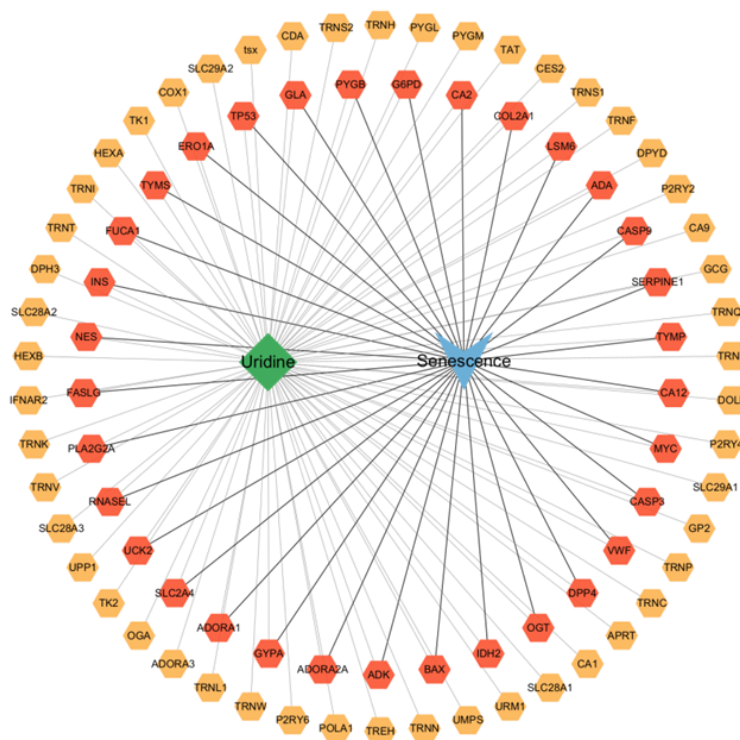


Fig. 2: Uridine-target-aging-related disease network.

3.1.2 Construction of active ingredient drug target interactions

Using Cytoscape 3.9.1 software to construct an "active ingredient target" graph for the treatment of age-related diseases with uridine. The green square mark represents the drug uridine, the blue arrow mark represents aging related diseases, the orange and yellow marks represent targets, and the gray connecting line indicates the interaction relationship (Fig. 2).

3.2 PPI network construction co expression gene network diagram

Using STRING database (<https://string-db.org>), the 33 intersecting gene targets of uridine aging related diseases obtained from the Venn diagram were imported, and the unrelated proteins were hidden to obtain a preliminary network protein map with 30 nodes, 85 edges, and a confidence value of 0.4. In Fig. 3, there are 4 red targets; 8 orange targets; and 18 yellow targets, sorted by degree in the following order: red targets > orange targets > yellow targets.

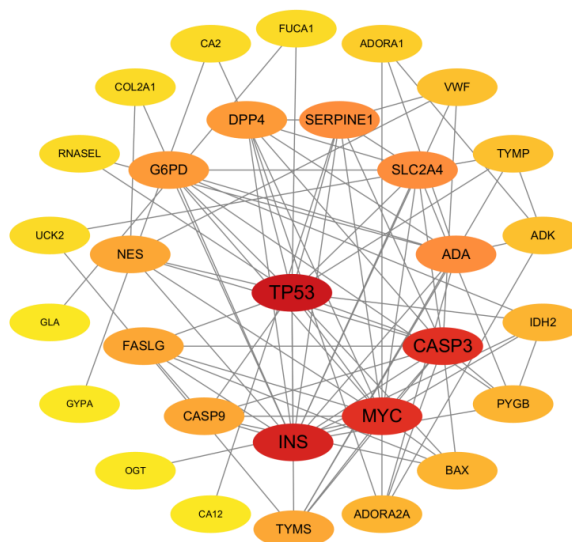


Fig. 3: Cytoscape, PPI network, potential target of uridine in the treatment of aging-related disease.

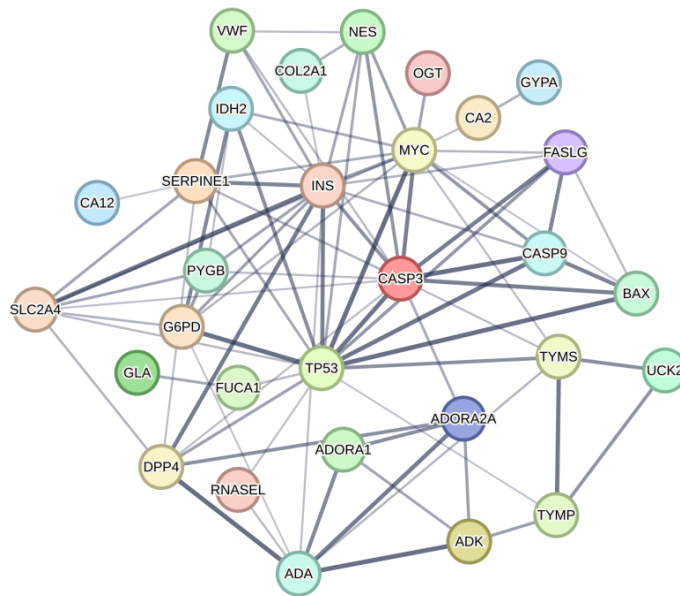


Fig 4: String, PPI network, potential target of uridine in the treatment of aging-related diseases.

Conducting PPI network analysis, 10 core targets are identified in the PPI network (Fig. 4), which are TP53 (light green target), INS (light pink target), CASP3 (red target), MYC (yellow target), ADA (light blue target), SERPINE1 (light orange target), SLC2A4 (light orange target), DPP4 (yellow target), G6PD (light orange target), and TYMS (yellow-green target).

3.3 GO enrichment analysis

GO functional enrichment analysis was performed on 33

intersecting targets using the Metascape platform, resulting in a total of 146 GO entries ($P < 0.5$). Among them, there are 55 entries related to biological processes, mainly involving the process of leukocyte apoptosis, regulation of neuronal apoptosis, regulation of apoptosis signaling pathways, apoptosis of glial cells, positive regulation of neuronal apoptosis, *etc*; 50 entries related to cellular components, including vesicles, secretory granules, lysosomes, *etc*. There are 41 entries related to molecular functions, covering functions such as protease binding, cytokine receptor binding, and signal receptor regulatory activity (Fig. 5).

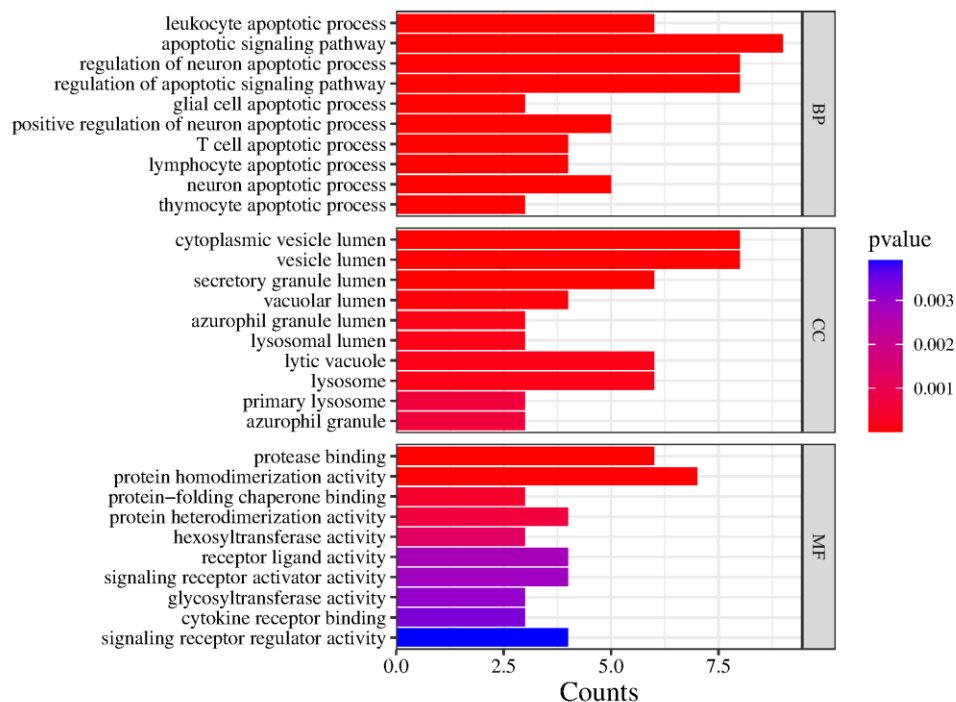


Fig. 5: GO enrichment analysis of key targets of uridine in anti-aging-related diseases.

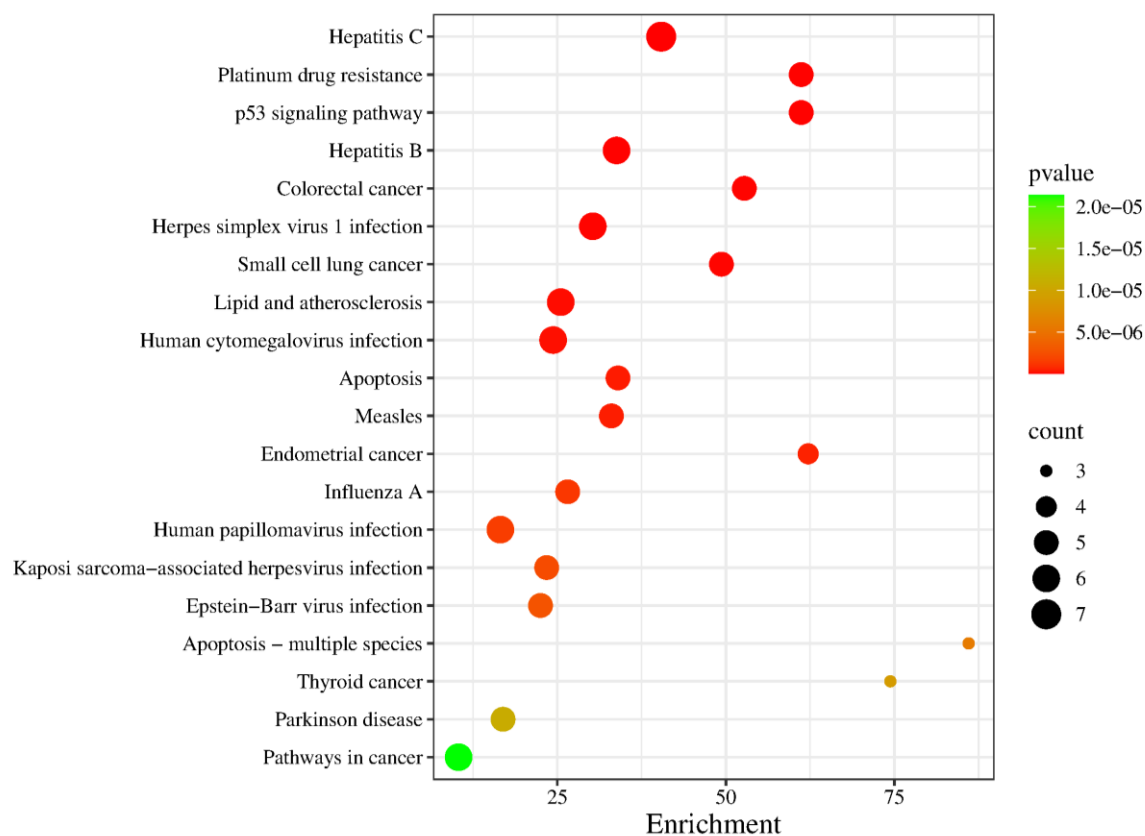


Fig. 6: KEGG enrichment analysis of key targets for uridine anti-aging-related diseases.

3.4 KEGG pathway enrichment analysis

The enrichment analysis of KEGG pathway was carried out on the Metascape platform for 33 intersection targets, and the results included 103 signal pathways ($P < 0.5$). TP53, or tumor protein p53, primarily functions by responding to cellular stress responses such as DNA damage, hypoxia, and metabolic stress, regulating the expression of various downstream genes. TP53 is involved in cell cycle regulation, DNA damage repair, apoptosis, and senescence processes. Mutations in TP53 are related to the occurrence and progression of various human cancers, and these mutations can impair its tumor-suppressive function.^[24] CASP3 (Caspase-3) is a cysteine-aspartic protease that plays a key role in the apoptosis process and is widely used as a biomarker for apoptosis; it is involved in the cleavage of amyloid precursor proteins and is associated with neuronal death.^[25] Insulin has the function of lowering blood glucose concentration; it increases the permeability of cells to monosaccharides, amino acids, and fatty acids, and it can also accelerate glycolysis, the pentose phosphate pathway, and glycogen synthesis in the liver.^[26] KEGG pathway enrichment analysis has also confirmed this conclusion. The results included 103 signal pathways ($P < 0.5$). According to the P value, it mainly focused on cancer related pathways, Parkinson disease related pathways, lipid and atherosclerosis,

P53 signal pathways and other pathways closely related to aging related diseases (Fig. 6).

3.5 Molecular docking

Molecular docking validation was performed on uridine with 10 core targets (TP53, INS, CASP3, MYC, ADA, SERPINE1, SLC2A4, DPP4, G6PD, and TYMS), as shown in Fig. 7. The lower the binding energy, the stronger the affinity between the ligand and the receptor, and the more stable the conformation.^[27] All docking results have binding energies less than -2 kcal/mol, indicating good binding between the core target and key components, as shown in Fig. 8). G6PD, SERPINE1, and ADA were selected for visualization (Fig. 7).

3.6 Protective effect of uridine on aging HT22, BV2, and PC12 cells

3.6.1 CCK-8 detection of cell viability and toxicity

3.6.1.1 Effects of different concentrations D-galactose on three cell activities

Compared with the control group, when the concentration of D-galactose was 10-100 mM/mL ($P < 0.01$), the viability of HT22, BV2, and PC12 cells showed a significant decrease trend, reaching the lowest at 100 mM/mL.^[28] Among them, the cell viability decreased to around 50% at 50 mM/mL, and the cell viability remained around 50% at both 50 mM and 100

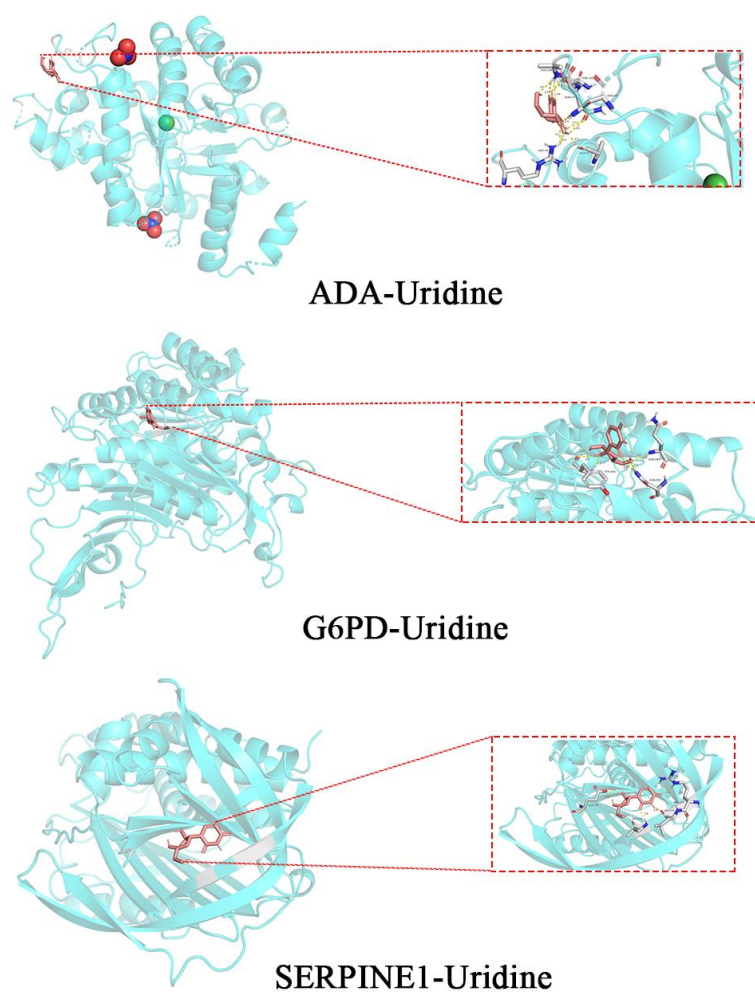


Fig. 7: ADA, G6PD, SERPINE1 visualized with uridine.

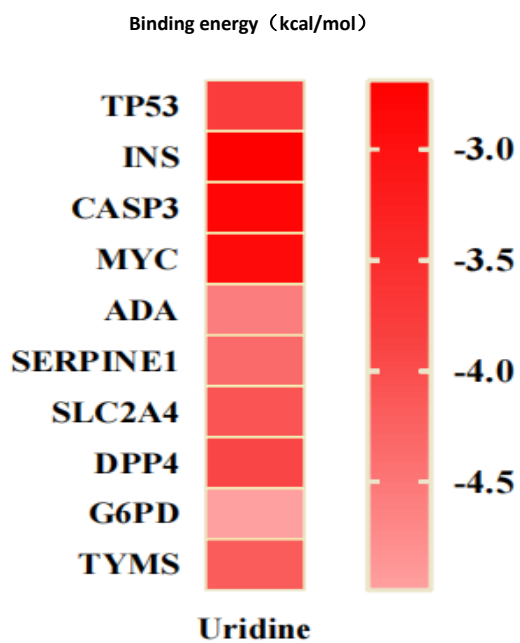


Fig. 8: Molecular docking binding energy heat map.

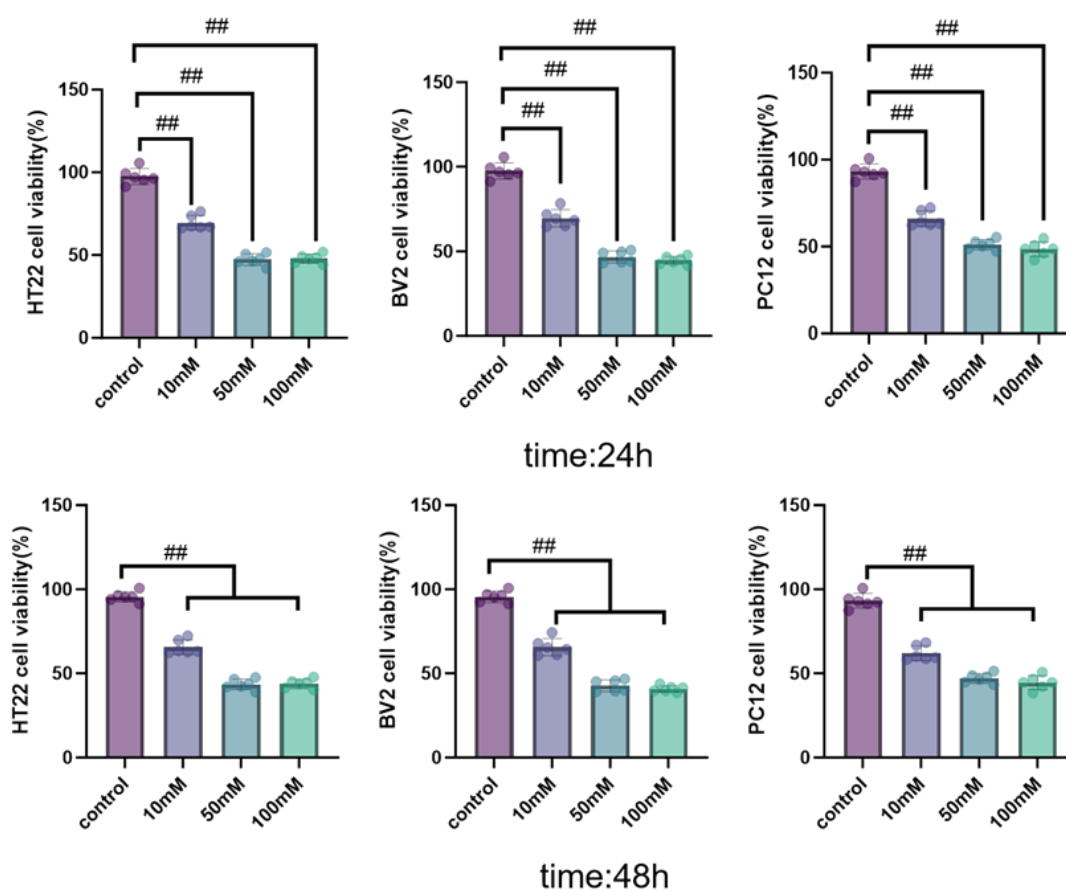


Fig. 9: Survival of HT22, BV2, and PC12 cells after modeling at different concentrations of D-galactose. Note: Compared with the control group, ## $P < 0.01$.

mM concentrations of D-galactose, with little change. Therefore, the modeling concentration for subsequent experiments was selected as 50 mM/mL ($P < 0.01$) (Fig. 9).

3.6.1.2 Screening of safe concentration range for uridine

Compared to the blank control group (the blank control group consists of culture medium + cells), as the concentration of

uridine continued to increase (20-60 $\mu\text{M}/\text{mL}$), the cell viability of HT22, BV2, and PC12 cells increased. This indicates that uridine has almost no cytotoxicity, is relatively safe, and has a significant proliferative effect. As shown in Fig. 10, compared with the control group, the cell survival rates of HT22, BV2, and PC12 cells increased slightly when the uridine concentration was 20 $\mu\text{M}/\text{mL}$. Increasing the uridine

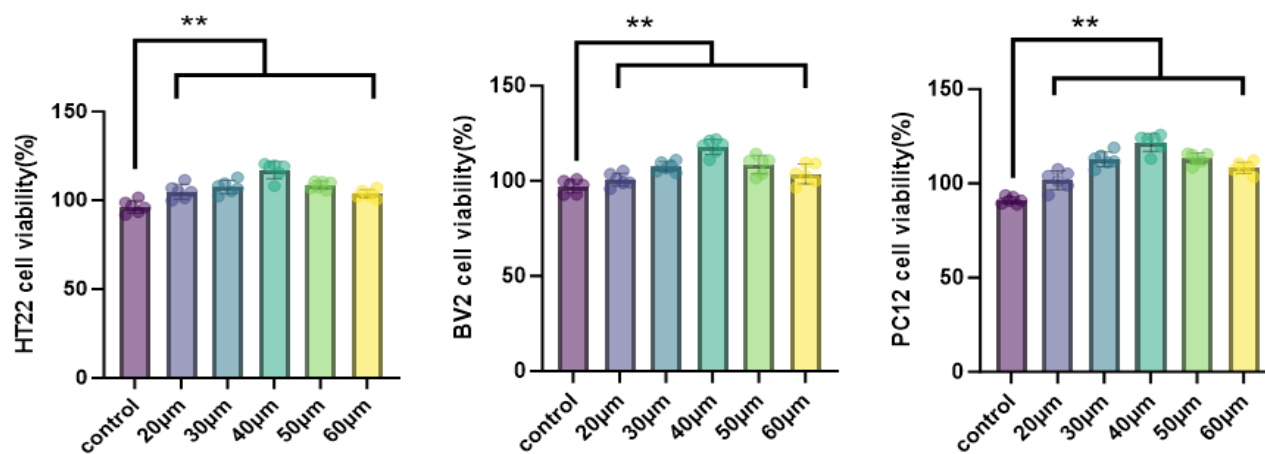


Fig. 10: HT22, BV2, and PC12 cell viability after administration of different concentrations of uridine. Note: Compared with the control group, ** $P < 0.01$.

concentration to 30 $\mu\text{M}/\text{mL}$ resulted in a more significant proliferation effect and the highest cell survival rate was reached at 40 $\mu\text{M}/\text{mL}$. Continuing to increase the uridine concentration resulted in a decrease in cell survival rate. Therefore, 20 $\mu\text{M}/\text{mL}$, 30 $\mu\text{M}/\text{mL}$, and 40 $\mu\text{M}/\text{mL}$ were designated as the low-dose group (L), medium dose group (M), and high-dose group (H) of uridine ($P < 0.01$).

3.6.1.3 Therapeutic effect of uridine on aging cells

50 mM/mL D-galactose was selected for modeling, and after 24 hours of modeling, 20 $\mu\text{M}/\text{mL}$, 30 $\mu\text{M}/\text{mL}$, and 40 $\mu\text{M}/\text{mL}$ uridine were added for treatment. The therapeutic effect is shown in the following figure. In HT22, BV2, and PC12 cells, compared with the blank group, the cell survival rate of the model group decreased significantly to below 50%, proving the successful establishment of the model. After modeling, treatment with low, medium, and high doses of uridine was given. The low-dose and medium dose uridine groups could restore the cell survival rate to 70%, while the high-dose uridine group could restore the cell survival rate to 80% ($P < 0.01$). This proves that uridine has a significant therapeutic

effect on D-galactose-induced aging of HT22, BV2, and PC12 cells (Fig 11). The results showed that pre-treatment with uridine increased the cell viability of HT22, BV2, and PC12 cells induced by D-galactose, reduced cell damage, and inhibited D-galactose-induced cell senescence. Uridine has a significant therapeutic effect on D-galactose-induced aging of HT22, BV2, and PC12 cells.

3.6.2 Biochemical index detection results

3.6.2.1 Uridine on the levels of MDA, LDH, and SOD in HT22, BV2, and PC12 cells

As shown in Figs. 12-14, HT22, BV2, and PC12 cells stimulated with D-galactose showed a significant increase in MDA content and LDH enzyme activity compared to the blank group ($P < 0.05$), while SOD enzyme activity decreased significantly ($P < 0.05$). After 24 hours of treatment with low, medium, and high doses of uridine, compared with the model group, the MDA content and LDH enzyme activity of the three types of cells significantly decreased ($P < 0.01$), and the SOD enzyme activity significantly increased ($P < 0.05$).

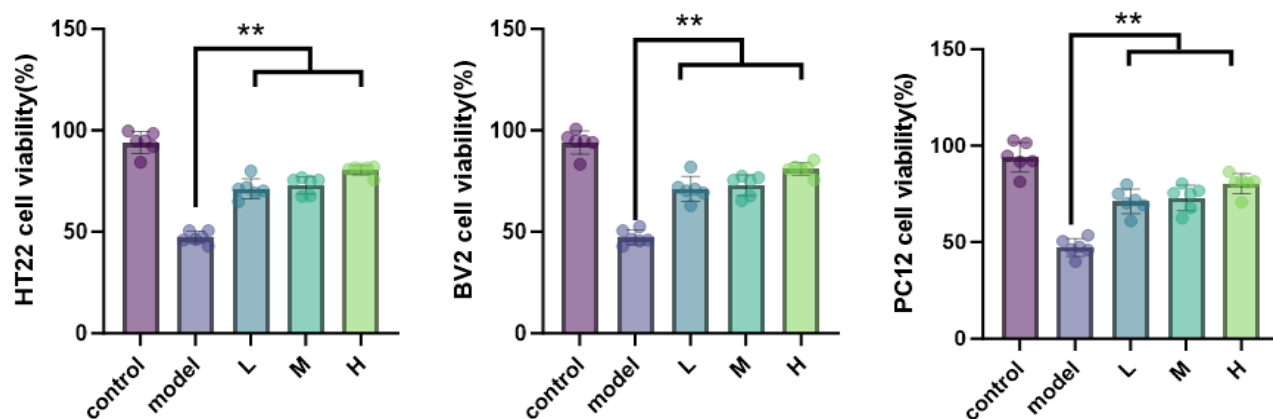


Fig. 11: Cell viability of HT22, BV2, and PC12 cells after 50 mM/mL D-galactose modeling and uridine treatment. Note: Compared with the model group, $**P < 0.01$.

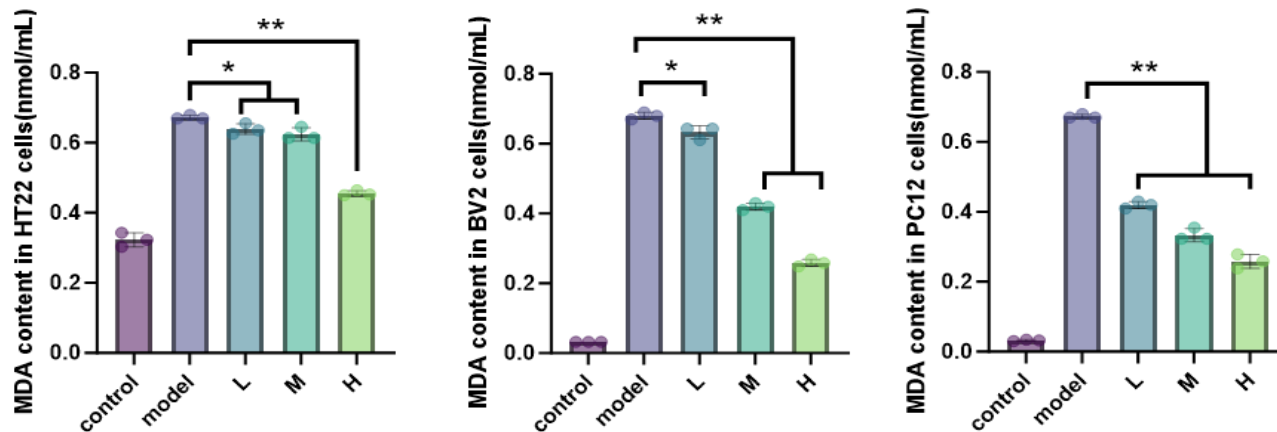


Fig. 12: Effect of uridine on MDA levels in HT22, BV2, and PC12 cells. Note: Compared with the model group, $*P < 0.05$, $**P < 0.01$.

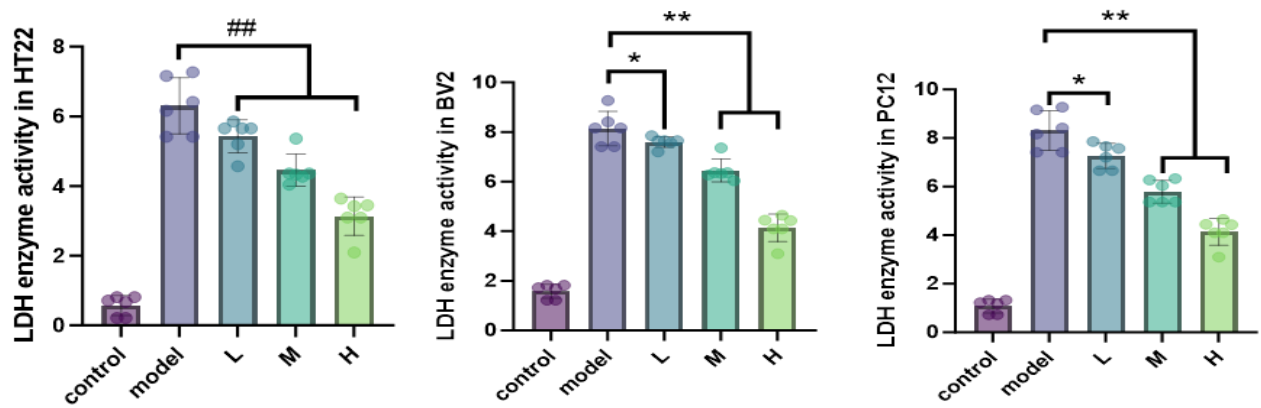


Fig. 13: Effect of uridine on LDH levels in HT22, BV2, and PC12 cells. Note: Compared with the model group, * $P < 0.05$, ** $P < 0.01$.

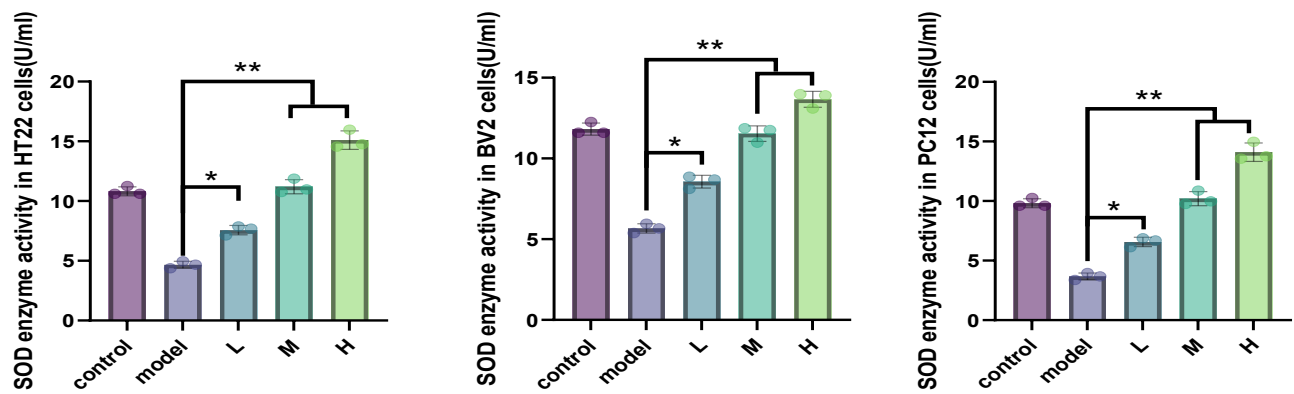


Fig. 14: Effect of uridine on SOD levels in HT22, BV2, and PC12 cells. Note: Compared with the model group, * $P < 0.05$, ** $P < 0.01$.

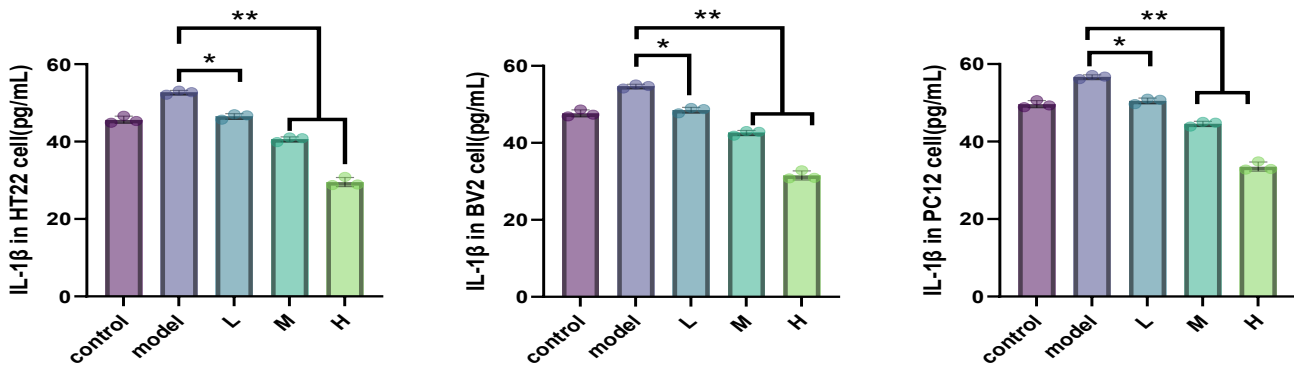


Fig. 15: Effect of uridine on IL-1 β content in HT22, BV2, and PC12 cells. Note: Compared with the model group, * $P < 0.05$, ** $P < 0.01$.

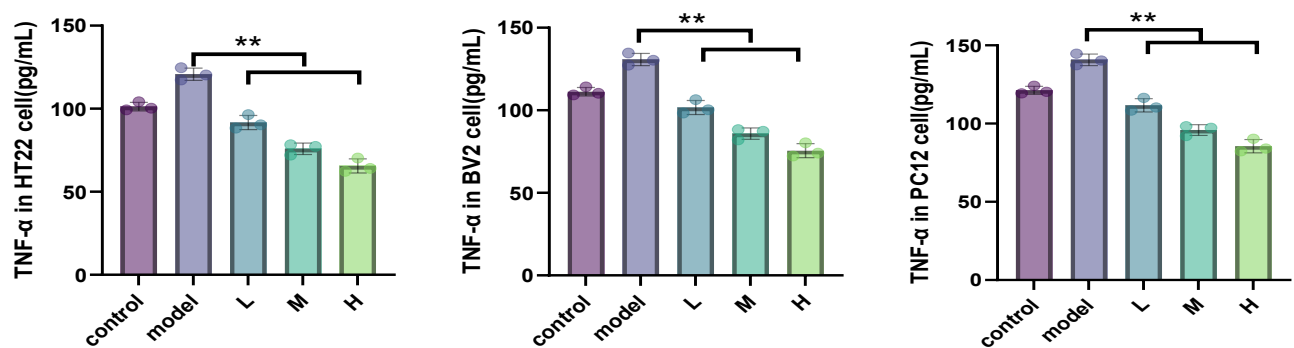


Fig. 16: Effect of uridine on TNF- α content in HT22, BV2, and PC12 cells. Note: Compared with the model group, * $P < 0.05$, ** $P < 0.01$.

3.6.2.2 The levels of TNF- α and IL-1 β in HT22, BV2, and PC12 cells

Compared with the blank group, HT22, BV2, and PC12 cells stimulated with D-galactose showed a significant increase in TNF- α and IL-1 β levels. After 24 hours of treatment with low, medium, and high doses of uridine, the levels of TNF- α and IL-1 β in the three types of cells significantly decreased compared to the model group. Uridine can reduce the expression levels of IL-1 β and TNF- α inflammatory factors, and reduce the damage of HT22, BV2, and PC12 cells to inflammatory factors ($P < 0.05$) (Figs. 15 and 16).

4. Discussion

Aging is a physiological process in which the body's ability to adapt decreases with age, ultimately leading to its failure or even death.^[29,30] Aging is influenced by various comprehensive factors such as genetics, environment, and nutrition, and is usually manifested as skin aging, decreased digestive function, decreased metabolic capacity, and accompanied by various symptoms such as decreased brain cognitive ability.^[31-33] In recent years, with the progress of social development and continuous economic growth, people's daily lives have become increasingly fast-paced, and the birth rate has been decreasing year by year. The problem of population aging has become more and more serious.^[34,35] More than 78% of elderly people suffer from at least one chronic disease, and the number of disabled elderly people continues to increase.^[36,37] The continuous increase in the elderly population has brought great burden to social healthcare. Currently, there are still limited strategies and intervention methods for delaying aging, and it is urgent to explore and develop new anti-aging drugs.^[38,39]

Uridine is a small molecule monomer of nucleoside, with a high content of 0.6557 mg·g⁻¹ in nucleoside components. Uridine is a type B monoamine oxidase inhibitor with anti-aging effects.^[40,41] Uridine can regulate enzymes and intermediates in uridine metabolism, thereby affecting intracellular glucose homeostasis, lipid metabolism, and amino acid metabolism.^[42,43] Uridine, as a key metabolite in anti-aging, can restore the vitality of aging human stem cells and promote the regeneration of various tissues in the body.^[44,45]

Then GO functional enrichment analysis was performed on 33 intersecting targets, and the relevant entries obtained mainly involved the process of leukocyte apoptosis, regulation of neuronal apoptosis, regulation of apoptosis signaling pathways, glial cell apoptosis, positive regulation of neuronal apoptosis, vesicles, secretory granules, lysosomes, protease binding, cytokine receptor binding, and signal receptor regulatory activity, all of which are related to aging.

The KEGG pathway enrichment analysis results mainly focus on cancer related pathways, Parkinson disease related pathways, lipid and atherosclerosis, P53 signaling pathways and other pathways closely related to aging related diseases. Subsequently, uridine was validated by molecular docking with 10 core targets (TP53, INS, CASP3, MYC, ADA,

SERPINE1, SLC2A4, DPP4, G6PD, and TYMS). The lower the binding energy, the stronger the affinity between the ligand and the receptor, and the more stable the conformation. All docking results have binding energies less than -2kcal/mol, indicating good binding between the core target and key components. Then, the anti-aging effect of uridine was verified through cell experiments. Due to the fact that the nervous system is one of the most affected systems by aging in the human body, we selected three types of cells, HT-22, BV2, and PC12, for validation. Using D-galactose to induce an aging cell model, treatment with uridine significantly improved cell survival rate. After uridine treatment, the MDA content and LDH enzyme activity in HT22, BV2, and PC12 cells were significantly reduced, while SOD enzyme activity was increased, and the expression levels of IL-1 β and TNF- α inflammatory factors were reduced. Therefore, this article verifies the anti-aging effect of uridine through network pharmacology, molecular docking, and cell experiments.

5. Conclusion

The research results show that uridine can exert anti-aging effects by regulating multiple targets and signaling pathways, especially demonstrating significant protective effects in nervous system cells. Firstly, 33 gene targets are potential targets for uridine treatment of age-related diseases. Subsequently, a coexpressed gene network diagram-PPI network diagram was constructed, and 10 core targets were screened in the PPI network. GO functional enrichment analysis was performed all of which are related to aging. The KEGG pathway enrichment analysis results mainly focus on pathways closely related to aging related diseases. This provides a theoretical basis and experimental support for the development of new anti-aging drugs. This study comprehensively employed a variety of technical means, from network pharmacology to molecular docking and then to cell experiments, to systematically verify the anti-aging potential of uridine. In the future, the possibility of its clinical application can be further explored to provide new ideas for addressing the health challenges brought about by population aging.

Acknowledgments

The authors gratefully acknowledge “Caiyun Postdoctoral Program” of innovation project 2023 that provides financial support for this work.

Conflict of Interest

There is no conflict of interest.

Supporting Information

Not applicable.

References

[1] C. Y. Ho, O. Dreesen, Faces of cellular senescence in skin aging, *Mechanisms of Ageing and Development*, 2021, **198**,

- 111525, doi: 10.1016/j.mad.2021.111525.
- [2] A. Calcinotto, J. Kohli, E. Zagato, L. Pellegrini, M. Demaria, A. Alimonti, Cellular senescence: aging, cancer, and injury, *Physiological Reviews*, 2019, **99**, 1047-1078, doi: 10.1152/physrev.00020.2018.
- [3] A. C. Franco, C. Aveleira, C. Cavadas, Skin senescence: mechanisms and impact on whole-body aging, *Trends in Molecular Medicine*, 2022, **28**, 97-109, doi: 10.1016/j.molmed.2021.12.003.
- [4] P. Gupta, S. Biswas, A. K. Chaturvedi, U. Janghel, G. Tamrakar, R. Verma, M. Hait, Health impact of ground water sample and its effect on flora of kanker district, chhattisgarh, India, *ES Food & Agroforestry*, 2023, **13**, 940, doi: 10.30919/esfaf940.
- [5] W. E. Sawyer, S. C. Izah, Unmasking food adulteration: public health challenges, impacts and mitigation strategies, *ES General*, 2024, **4**, 1091, doi: 10.30919/esg1091.
- [6] A. Hernandez-Segura, J. Nehme, M. Demaria, Hallmarks of cellular senescence, *Trends in Cell Biology*, 2018, **28**, 436-453, doi: 10.1016/j.tcb.2018.02.001.
- [7] R. Liu, Aging, cellular senescence, and Alzheimer's disease, *International Journal of Molecular Sciences*, 2022, **23**, 1989, doi: 10.3390/ijms23041989.
- [8] A. Guerrero, B. De Strooper, I. L. Arancibia-Cárcamo, Cellular senescence at the crossroads of inflammation and Alzheimer's disease, *Trends in Neurosciences*, 2021, **44**, 714-727, doi: 10.1016/j.tins.2021.06.007.
- [9] H. Pei, X. Dai, Z. He, Z. Tang, Y. Zhu, R. Du, PM_{2.5} exposure promotes the progression of acute kidney injury by activating NLRP3-mediated macrophage inflammatory response, *Ecotoxicology and Environmental Safety*, 2024, **278**, 116454, doi: 10.1016/j.ecoenv.2024.116454.
- [10] H. Luo, Y. Li, H. Song, K. Zhao, W. Li, H. Hong, Y. Wang, L. Qi, Y. Zhang, Role of EZH2-mediated epigenetic modification on vascular smooth muscle in cardiovascular diseases: a mini-review, *Frontiers in Pharmacology*, 2024, **15**, 1416992, doi: 10.3389/fphar.2024.1416992.
- [11] H. Pei, H. Shen, J. Bi, Z. He, L. Zhai, Gastrodin improves nerve cell injury and behaviors of depressed mice through Caspase-3-mediated apoptosis, *CNS Neuroscience & Therapeutics*, 2024, **30**, e14444, doi: 10.1111/cns.14444.
- [12] G. Zaffagnini, S. Cheng, M. C. Salzer, B. Pernaute, J. M. Duran, M. Irimia, M. Schuh, E. Böke, Mouse oocytes sequester aggregated proteins in degradative super-organelles, *Cell*, 2024, **187**, 1109-1126, doi: 10.1016/j.cell.2024.01.031.
- [13] Y. Yang, X. Lu, N. Liu, S. Ma, H. Zhang, Z. Zhang, K. Yang, M. Jiang, Z. Zheng, Y. Qiao, Q. Hu, Y. Huang, Y. Zhang, M. Xiong, L. Liu, X. Jiang, P. Reddy, X. Dong, F. Xu, Q. Wang, Q. Zhao, J. Lei, S. Sun, Y. Jing, J. Li, Y. Cai, Y. Fan, K. Yan, Y. Jing, A. Haghani, M. Xing, X. Zhang, G. Zhu, W. Song, S. Horvath, C. Rodriguez Esteban, M. Song, S. Wang, G. Zhao, W. Li, J. C. Izpisua Belmonte, J. Qu, W. Zhang, G. Liu, Metformin decelerates aging clock in male monkeys, *Cell*, 2024, **187**, 6358-6378, doi: 10.1016/j.cell.2024.08.021.
- [14] Q. Qu, Y. Chen, Y. Wang, S. Long, W. Wang, H. Yang, M. Li, X. Tian, X. Wei, Y. Liu, S. Xu, C. Zhang, M. Zhu, S. M. Lam, J. Wu, C. Yun, J. Chen, S. Xue, B. Zhang, Z. Zheng, H. Piao, C. Jiang, H. Guo, G. Shui, X. Deng, C. Zhang, S. Lin, Lithocholic acid phenocopies anti-ageing effects of calorie restriction, *Nature*, 2025, **643**, 192-200, doi: 10.1038/s41586-024-08329-5.
- [15] B. G. Childs, M. Durik, D. J. Baker, J. M. van Deursen, Cellular senescence in aging and age-related disease: from mechanisms to therapy, *Nature Medicine*, 2015, **21**, 1424-1435, doi: 10.1038/nm.4000.
- [16] D. McHugh, J. Gil, Senescence and aging: Causes, consequences, and therapeutic avenues, *The Journal of Cell Biology*, 2018, **217**, 65-77, doi: 10.1083/jcb.201708092.
- [17] D. J. Baker, B. G. Childs, M. Durik, M. E. Wijers, C. J. Sieben, J. Zhong, R. A. Saltness, K. B. Jeganathan, G. C. Verzosa, A. Pezeshki, K. Khazaie, J. D. Miller, J. M. van Deursen, Naturally occurring p16Ink4a-positive cells shorten healthy lifespan, *Nature*, 2016, **530**, 184-189, doi: 10.1038/nature16932.
- [18] Z. C. Nwosu, M. H. Ward, P. Sajjakulnukit, P. Poudel, C. Ragulan, S. Kasperek, M. Radyk, D. Sutton, R. E. Menjivar, A. Andren, J. J. Apiz-Saab, Z. Tolstyka, K. Brown, H.-J. Lee, L. N. Dzierzynski, X. He, H. Ps, J. Ugras, G. Nyamundanda, L. Zhang, C. J. Halbrook, E. S. Carpenter, J. Shi, L. P. Shriver, G. J. Patti, A. Muir, M. Pasca di Magliano, A. Sadanandam, C. A. Lyssiotis, Uridine-derived ribose fuels glucose-restricted pancreatic cancer, *Nature*, 2023, **618**, 151-158, doi: 10.1038/s41586-023-06073-w.
- [19] S. He, N. E. Sharpless, Senescence in health and disease, *Cell*, 2017, **169**, 1000-1011, doi: 10.1016/j.cell.2017.05.015.
- [20] X. Bai, D. Huang, P. Xie, R. Sun, H. Zhou, Y. Liu, Effect of uridine on mitochondrial function, *Sheng Wu Gong Cheng Xue Bao*, 2023, **39**: 3695-3709, doi: 10.13345/j.cjb.220899.
- [21] J. P. de Magalhães, Cellular senescence in normal physiology, *Science*, 2024, **384**, 1300-1301, doi: 10.1126/science.adj7050.
- [22] W. Yu, X. Li, Q. Sun, S. Yi, G. Zhang, L. Chen, Z. Li, J. Li, L. Luo, Metabolomics and network pharmacology reveal the mechanism of Castanopsis honey against *Streptococcus pyogenes*, *Food Chemistry*, 2024, **441**, 138388, doi: 10.1016/j.foodchem.2024.138388.
- [23] A. N. Kristanti, N. S. Aminaha, I. Siswanto, A. P. Wardana, M. I. Abdjan, A. R. Khoirunisak, E. Noviana, Synthesis, pharmacokinetic, molecular docking, and molecular dynamics simulation of 2-styrylchromone derivatives as potential inhibitor of human kinesin Eg5, *Engineered Science*, 2024, **30**, 1168, doi: 10.30919/es1168.
- [24] M. B. Mansur, M. Greaves, Convergent TP53 loss and evolvability in cancer, *BMC Ecology and Evolution*, 2023, **23**, 54, doi: 10.1186/s12862-023-02146-6.
- [25] M. Linder, T. Tschernig, Vasculogenic mimicry: Possible role of effector caspase-3, caspase-6 and caspase-7, *Anatomischer Anzeiger*, 2016, **204**, 114-117, doi: 10.1016/j.aanat.2015.11.007.
- [26] K. D. Niswender, Basal insulin: physiology, pharmacology, and clinical implications, *Postgraduate Medicine*, 2011, **123**, 17-26, doi: 10.3810/pgm.2011.07.2300.
- [27] Y. Dong, B. Tao, X. Xue, C. Feng, Y. Ren, H. Ma, J. Zhang, Y. Si, S. Zhang, S. Liu, H. Li, J. Zhou, G. Li, Z. Wang, J. Xie, Z.

- Zhu, Molecular mechanism of Epicedium treatment for depression based on network pharmacology and molecular docking technology, *BMC Complementary Medicine and Therapies*, 2021, **21**, 222, doi: 10.1186/s12906-021-03389-w.
- [28] Q. Lou, X. Meng, C. Wei, J. Tong, Y. Chen, M. Li, Q. Wang, S. Guo, J. Duan, E. Shang, Y. Zhu, Jian-Yan-Ling capsules ameliorate cognitive impairment in mice with D-galactose-induced senescence and inhibit the oxidation-induced apoptosis of HT22 hippocampal cells by regulating the Nrf2-HO1 signaling pathway, *Journal of Ethnopharmacology*, 2023, **310**, 116356, doi: 10.1016/j.jep.2023.116356.
- [29] M. J. Regulski, Cellular senescence: What, why, and how, *Wounds*, 2017, **29**, 168-174.
- [30] N. S. Mohamad Kamal, S. Safuan, S. Shamsuddin, P. Foroozandeh, Aging of the cells: Insight into cellular senescence and detection Methods, *European Journal of Cell Biology*, 2020, **99**, 151108, doi: 10.1016/j.ejcb.2020.151108.
- [31] R. Du, H. Pei, Z. He, J. Wang, X. Zhou, W. Li, D. Zhu, C. Zhang, Astragalin improves cognitive disorder in Alzheimer's disease: Based on network pharmacology and molecular docking simulation, *CNS Neuroscience & Therapeutics*, 2024, **30**, e14799, doi: 10.1111/cns.14799.
- [32] J. Birch, J. Gil, Senescence and the SASP: many therapeutic avenues, *Genes & Development*, 2020, **34**, 1565-1576, doi: 10.1101/gad.343129.120.
- [33] L. Zhang, L. E. Pitcher, M. J. Yousefzadeh, L. J. Niedernhofer, P. D. Robbins, Y. Zhu, Cellular senescence: a key therapeutic target in aging and diseases, *The Journal of Clinical Investigation*, 2022, **132**, e158450, doi: 10.1172/JCI158450.
- [34] W. Tao, Z. Yu, J. J. Han, Single-cell senescence identification reveals senescence heterogeneity, trajectory, and modulators, *Cell Metabolism*, 2024, **36**, 1126-1143, doi: 10.1016/j.cmet.2024.03.009.
- [35] B. Wang, J. Han, J. H. Elisseff, M. Demaria, The senescence-associated secretory phenotype and its physiological and pathological implications, *Nature Reviews Molecular Cell Biology*, 2024, **25**, 958-978, doi: 10.1038/s41580-024-00727-x.
- [36] N. Rex, A. Melk, R. Schmitt, Cellular senescence and kidney aging, *Clinical Science*, 2023, **137**, 1805-1821, doi: 10.1042/cs20230140.
- [37] Q. Zeng, Y. Gong, N. Zhu, Y. Shi, C. Zhang, L. Qin, Lipids and lipid metabolism in cellular senescence: Emerging targets for age-related diseases, *Ageing Research Reviews*, 2024, **97**, 102294, doi: 10.1016/j.arr.2024.102294.
- [38] L. Melo dos Santos, M. Trombetta-Lima, B. Eggen, M. Demaria, Cellular senescence in brain aging and neurodegeneration, *Ageing Research Reviews*, 2024, **93**, 102141, doi: 10.1016/j.arr.2023.102141.
- [39] M. V. Blagosklonny, Cell senescence, rapamycin and hyperfunction theory of aging, *Cell Cycle*, 2022, **21**, 1456-1467, doi: 10.1080/15384101.2022.2054636.
- [40] C. A. Arbour, B. Imperiali, Uridine natural products: Challenging targets and inspiration for novel small molecule inhibitors, *Bioorganic & Medicinal Chemistry*, 2020, **28**, 115661, doi: 10.1016/j.bmc.2020.115661.
- [41] G. P. Connolly, J. A. Duley, Uridine and its nucleotides: biological actions, therapeutic potentials, *Trends in Pharmacological Sciences*, 1999, **20**, 218-225, doi: 10.1016/S0165-6147(99)01298-5.
- [42] T. Yamamoto, H. Koyama, M. Kurajoh, T. Shoji, Z. Tsutsumi, Y. Moriwaki, Biochemistry of uridine in plasma, *Clinica Chimica Acta*, 2011, **412**, 1712-1724, doi: 10.1016/j.cca.2011.06.006.
- [43] W. V. Zheng, Y. Li, X. Cheng, Y. Xu, T. Zhou, D. Li, Y. Xiong, S. Wang, Z. Chen, Uridine alleviates carbon tetrachloride-induced liver fibrosis by regulating the activity of liver-related cells, *Journal of Cellular and Molecular Medicine*, 2022, **26**, 840-854, doi: 10.1111/jcmm.17131.
- [44] C. J. van Groeningen, G. J. Peters, H. M. Pinedo, Modulation of fluorouracil toxicity with uridine, *Seminars in Oncology*, 1992, **19**, 148-154.
- [45] U. A. Walker, N. Venhoff, Uridine in the prevention and treatment of NRTI-related mitochondrial toxicity, *Antiviral Therapy*, 2005, **10**, M117-M123.

Publisher's Note: Engineered Science Publisher remains neutral with regard to jurisdictional claims in published maps and institutional affiliations.

Open Access

This article is licensed under a Creative Commons Attribution 4.0 International License, which permits the use, sharing, adaptation, distribution and reproduction in any medium or format, as long as appropriate credit to the original author(s) and the source is given by providing a link to the Creative Commons license and changes need to be indicated if there are any. The images or other third-party material in this article are included in the article's Creative Commons license, unless indicated otherwise in a credit line to the material. If material is not included in the article's Creative Commons license and your intended use is not permitted by statutory regulation or exceeds the permitted use, you will need to obtain permission directly from the copyright holder. To view a copy of this license, visit <http://creativecommons.org/licenses/by/4.0/>.

©The Author(s) 2025